ELSEVIER

Sensors and Actuators A 68 (1998) 221–228

SENSORS AND ACTUATORS A PHYSICAL

Procedure for in-use calibration of triaxial accelerometers in medical applications

J.C. Lötters [a], J. Schipper [b], P.H. Veltink [c,*], W. Olthuis [d], P. Bergveld [d]

[a] Bronkhorst High-Tech, Nijverheidsstraat 1A, NL-7261 AK Ruurlo, Netherlands
[b] Ericsson EMN, Institutenweg 25, NL-7521 PH Enschede, Netherlands
[c] BMTI, University of Twente, PO Box 217, NL-7500 AE Enschede, Netherlands
[d] MESA Research Institute, University of Twente, PO Box 217, NL-7500 AE Enschede, Netherlands

Abstract

In the medical field triaxial accelerometers are used for the monitoring of movements. Unfortunately, the long-term use of accelerometers is limited by drift of the sensitivities and the offsets. Therefore, a calibration procedure is designed which allows in-use calibration of a triaxial accelerometer. This procedure uses the fact that the modulus of the acceleration vector measured with a triaxial accelerometer equals $1g$ under quasi-static conditions. The calibration procedure requires no explicit knowledge of the actual orientation of the triaxial accelerometer with respect to gravity and requires only quasi-static random movements. The procedure can be performed within several minutes. Considering practical applications, it is found possible to obtain an average error smaller than 3% (of 1 $[g]$) with the calibration procedure for inputs caused by 'standing straight and moving slightly' when the offsets only are estimated. For the input caused by the sequence that occurs when going to bed, it is found possible to obtain errors smaller than 3% for estimating all parameters.

Keywords: Calibration; Accelerometers; Parameter estimation; Monitoring of movement

1. Introduction

The monitoring of movement using triaxial accelerometers plays an important role in the medical field, e.g., for functional electrical stimulation (FES).

A significant problem with the use of accelerometers is the drift of the sensitivity and offset. For the current commercially available accelerometers, the drift of these parameters causes the need for calibration within periods in the order of hours, which seriously limits the duration of an uninterrupted movement registration of a patient. To solve the problem of the drift, a calibration procedure is sought with which it is possible to calibrate a triaxial accelerometer while it is in use, requiring only random movements without explicit knowledge of the orientation of the sensor and without making the patient perform specified movements.

The existing calibration methods for triaxial accelerometers can roughly be divided into two groups. The first group of calibration methods can be categorized as laboratory oriented [1,2]: gravity is applied twice to each axis of the device, so this method is unsuited for use in most practical situations. The second group of methods, which is often used in the field of robotics and aviation, makes use of additional sensors, like gyroscopes and sometimes even the global positioning system [3,4], and is therefore not immediately appropriate for medical applications.

In this paper, an in-use calibration procedure for a triaxial accelerometer is presented and some simulation and measurement results are described and discussed. It uses the fact that the modulus of the acceleration vector measured with a triaxial accelerometer equals $1g$ under quasi-static conditions. In contrast to the calibration procedures for uniaxial accelerometers, the calibration procedure requires no explicit knowledge of the actual orientation of the triaxial accelerometer and requires only quasi-static random movements [5].

2. Theory

In the static situation, the output voltage of a uniaxial accelerometer is a measure for the angle θ [rad] between the sensitive axis of the device and the direction of gravity. The

* Corresponding author. Tel.: +31-53-489-27-65; Fax: +31-53-489-22-87; E-mail: p.h.veltink@el.utwente.nl.

0924-4247/98/$19.00
PII S0924-4247(98)00049-1

parameters sensitivity and offset of a uniaxial accelerometer can be obtained by applying two different angles to the device: thus, two equations with two unknowns are obtained. Therefore, the triaxial accelerometer could be calibrated by keeping each axis under two different known angles θ with respect to gravity, as shown in Fig. 1, thus obtaining six equations with six unknowns. This is the minimum required set of equations to know the three different sensitivities s_x, s_y and s_z [V g^{-1}] and offsets o_x, o_y, o_z [V] of the device.

However, in an in-use situation, this method needs interaction with the patient: to calibrate the sensor, the patient should apply six different known angles θ to the part of the body where the accelerometer is attached. This is inconvenient for the patient and may be difficult to perform. Furthermore, when the accelerometer is in use, hardly any static situations will occur due to (small) movements of the patient. Therefore, a calibration method should be found which does not need patient interaction, which does not require explicit knowledge of the orientation of the triaxial accelerometer and which can discriminate between static and dynamic situations.

In Fig. 2 a schematic overview of such a calibration system is presented. The system consists of the triaxial accelerometer and electronic circuitry, a voltage to acceleration value converter and the actual calibration procedure. The calibration procedure consists of two parts: a quasi-static moments detector [6] and a parameter estimator [7]. The quasi-static moments detector is used to obtain a collection of quasi-static moments out of an arbitrary collection of output voltages. Quasi-static moments are moments in which the variance of the modulus of the three-dimensional acceleration vector measured by the accelerometer acceleration is small. The quasi-static moments detector discards all samples for which the degree of movement is larger than a certain threshold value T_v above 1g. The threshold value represents the maximally allowed variance of the modulus of the acceleration vector. The parameter estimator is used to obtain values of the sensitivities s_x, s_y and s_z [V g^{-1}] and offsets o_x, o_y, o_z [V] of the triaxial accelerometer out of a collection of quasi-static output voltages. It uses the fact that the modulus of the total acceleration vector measured with a triaxial accelerometer equals 1g under quasi-static conditions. When all six parameter values are known and regularly updated, the output voltage of the accelerometer will always be correctly converted into a corresponding acceleration value.

The operation principle of the quasi-static moments detector can be explained as follows. When the sensor signal is not changing over time, it can be assumed that the sensor is not moving, because a constant acceleration or an exact cancellation of acceleration and gravitational components during movements is not to be expected for prolonged periods of time during normal body movements. This characteristic feature can be used to discriminate between quasi-static and dynamic moments. A quasi-static moments detector was constructed by applying a high-pass filter with a cut-off frequency $f_c = 0.5$ Hz, a rectifier and a low-pass filter with a cut-off frequency $f_c = 0.5$ Hz to the signal of the triaxial accel-

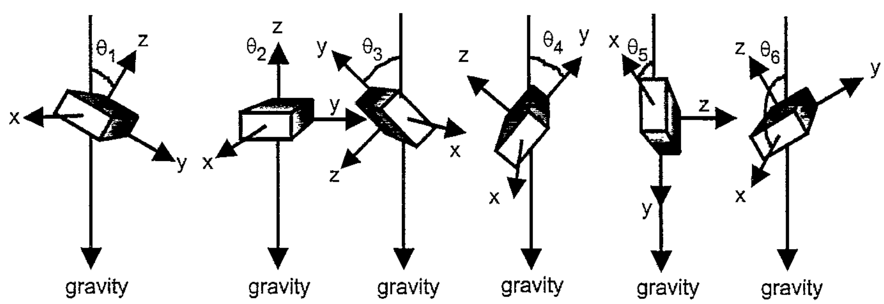

Fig. 1. Basic principle of the calibration procedure: the accelerometer is held under six different known angles θ vs. gravity.

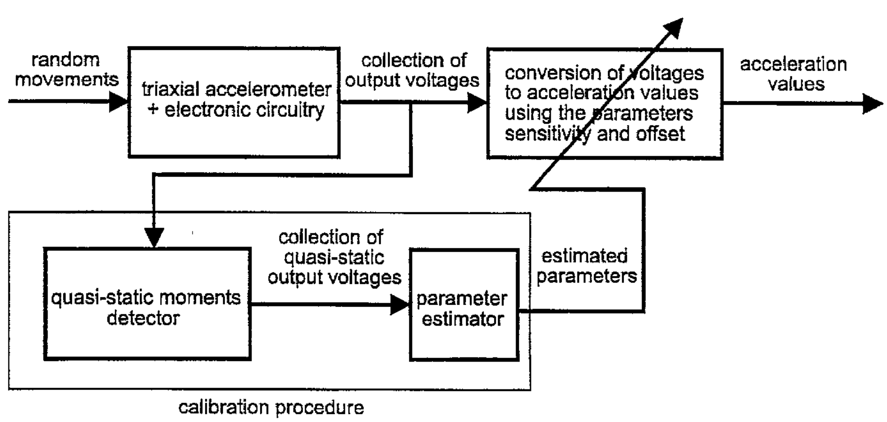

Fig. 2. Schematic representation of the calibration system.

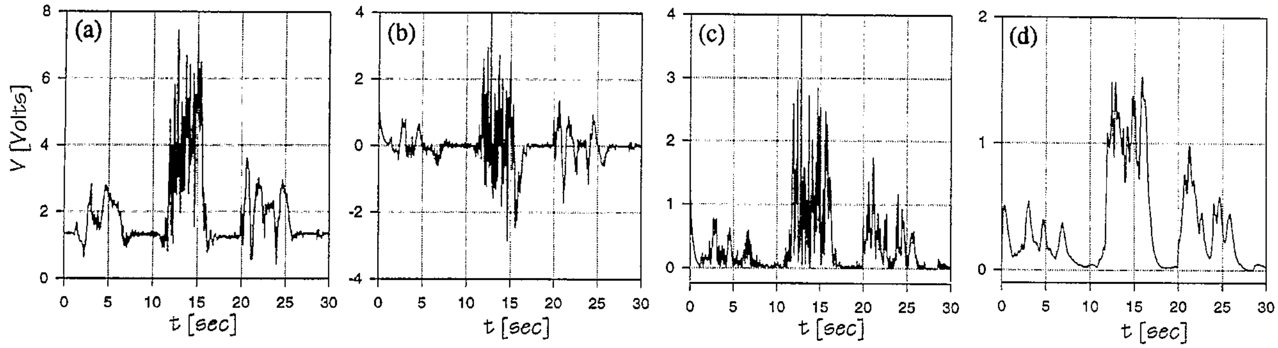

Fig. 3. Representation of the functioning of the static moments detector: (a) the composed accelerometer signal; (b) the signal after the high-pass filter; (c) the signal after the rectifier; (d) the signal after the low-pass filter.

erometer. A composition $v_{\mathrm{in,detection}}$ of the output voltages in the three orthogonal directions is created according to

$$v_{\mathrm{in,detection}}=\sqrt{v_x^2+v_y^2+v_z^2} \tag{1}$$

with v_x, v_y and v_z the output voltages of the accelerometer. Now, the quasi-static moments detector is applied to $v_{\mathrm{in,detection}}$ [V]. The resulting output voltage $v_{\mathrm{out,detection}}$ [V] can be equated to

$$v_{\mathrm{out,detection}}=\mathrm{LPF}(\mathrm{REC}(\mathrm{HPF}(v_{\mathrm{in,detection}}))) \tag{2}$$

To clarify the operation of each component of the detector, some random movements were performed with the triaxial accelerometer for a period of 30 s. The output voltages were registered and composed according to Eq. (1), as shown in Fig. 3(a). First, the high-pass filter was applied to $v_{\mathrm{in,detection}}$ (Fig. 3(b)), then the rectifier was applied (Fig. 3(c)) and finally the low-pass filter was applied (Fig. 3(d)).

It can be seen that the high-pass filter eliminates the offset, the rectifier creates an effective value and the low-pass filter smoothes the signal. The level of the output voltage of the quasi-static moments detector is a measure for the amount of movement that was present in the input signal. According to Ref. [6], the signal in Fig. 3(d) has to be compared to a threshold voltage T_v [V]. When the signal is smaller than the threshold voltage, the movement is static and otherwise dynamic. For the calibration procedure as described in this section,the optimum threshold value was experimentally found to be $T_v=0.40$ V [7].

There are a lot of estimation procedures [8]. The linear minimum variance unbiased estimator is chosen, because it requires little or no knowledge of the density functions of the random variables involved in the problem and the solution to non-linear problems can be well approximated by using linear theory.

The output voltage in each direction of the triaxial accelerometer can be described by

$$v_{\mathrm{dir}}=s_{\mathrm{dir}}\cdot a_{\mathrm{dir}}+o_{\mathrm{dir}} \tag{3}$$

with v [V] the output voltage, s [V g^{-1}] the sensitivity, a [g] the measured acceleration, o [V] the offset and dir the x-, y- or z-direction. In a certain period of time, a collection of output voltages is obtained. The collection of output voltages is supplied to a quasi-static moments detector with threshold value T_v which filters out most of the dynamic signals, thus leaving a collection of quasi-static output voltages. With this collection of quasi-static moments the parameter estimator is able to estimate the parameters of the sensor, which can intuitively be explained as follows. The collection of all possible static moments describes a sphere in the a_x-, a_y-, a_z-frame with the centre point at the frame's origin and with a radius of 1g, as shown in Fig. 4(a).

The triaxial accelerometer transforms the observed accelerations into voltages according to Eq. (3) and creates in the v_x-, v_y-, v_z-frame an ellipsoid with the centre point at the offset vector (o_x, o_y, o_z) and a radius of $s_x\cdot g$, $s_y\cdot g$ and $s_z\cdot g$ in the v_x-, v_y- and v_z-directions, respectively, as shown in Fig. 4(b). When gravity is the only occurring acceleration, the ellipsoid is mathematically described as in Eq. (4) below. By changing the parameters in such a way that for every point (v_x, v_y, v_z) Eq. (4) is satisfied, the parameters s_x, s_y, s_z, o_x, o_y and o_z can be found. The continuous adaptation of the parameters is performed by the parameter estimator.

$$\sqrt{\left(\frac{v_x-o_x}{s_x}\right)^2+\left(\frac{v_y-o_y}{s_y}\right)^2+\left(\frac{v_z-o_z}{s_z}\right)^2} \tag{4}$$

$$=1\ [g] \text{ in the static case!}$$

The general equation used to perform one estimation with the linear minimum variance unbiased estimator is [8]

$$y=h(\boldsymbol{v},\boldsymbol{p})+\mu \tag{5}$$

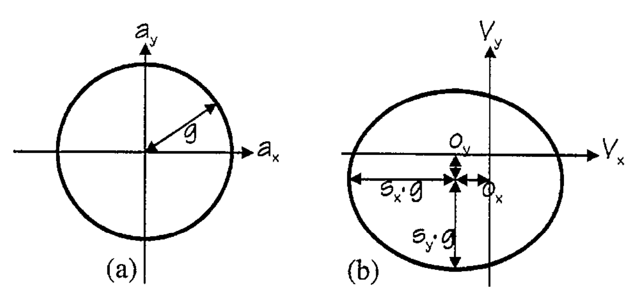

Fig. 4. Two-dimensional representation of all possible (a) static accelerations and (b) static voltages.

where y is the measured signal, $h(\boldsymbol{v},\boldsymbol{p})$ the mathematical model of the system to be calibrated as a function of the parameter vector $\boldsymbol{p}$, given by

$$\boldsymbol{p}=(s_x\ s_y\ s_z\ o_x\ o_y\ o_z) \tag{6}$$

and the input vector $\boldsymbol{v}$

$$\boldsymbol{v}=(v_x\ v_y\ v_z) \tag{7}$$

and μ the noise.

The mathematical model can be rewritten according to Eq. (4) as

$$h(\boldsymbol{v},\boldsymbol{p})=\sqrt{\left(\frac{v_x-o_x}{s_x}\right)^2+\left(\frac{v_y-o_y}{s_y}\right)^2+\left(\frac{v_z-o_z}{s_z}\right)^2} \tag{8}$$

In this paper, a slightly different interpretation is given to y. Usually, y is the measured value of the output. Here, however, y is assumed to be always 1 [g], which is true in the static case. The noise μ represents the deviations from 1 [g], caused by the fact that the collection of output voltages is not completely static but quasi-static.

Since the model $h(\boldsymbol{v},\boldsymbol{p})$ is a non-linear function of the elements of the parameter vector $\boldsymbol{p}$, the model is linearized by expanding it around a bias point which is determined with the 'previous estimation' [7]. It should be noted that the parameter vector needed for the first 'previous estimation' is provided by a pre-calibration step as schematically shown in Fig. 1 and described in Ref. [9]. The linearized mathematical model can be equated to

$$h(\boldsymbol{v},\boldsymbol{p})=h(\boldsymbol{v},\hat{\boldsymbol{p}}(-))+\frac{\partial h(\boldsymbol{v},\boldsymbol{p})}{\partial \boldsymbol{p}}\bigg|_{\boldsymbol{p}=\hat{\boldsymbol{p}}(-)}(\boldsymbol{p}-\hat{\boldsymbol{p}}(-))+\text{h.o.t.} \tag{9}$$

in which $\hat{\boldsymbol{p}}(-)$ is the previous estimated value of the parameter vector and h.o.t. represents the higher-order terms. By substituting Eq. (9) in Eq. (5) and by neglecting the higher-order terms, the following equation is derived:

$$y-h(\boldsymbol{v},\hat{\boldsymbol{p}}(-))=\frac{\partial h(\boldsymbol{v},\boldsymbol{p})}{\partial \boldsymbol{p}}\bigg|_{\boldsymbol{p}=\hat{\boldsymbol{p}}(-)}(\boldsymbol{p}-\hat{\boldsymbol{p}}(-))+\mu \tag{10}$$

The unknown parameter vector $\boldsymbol{p}$ can be estimated by solving Eq. (10) with the linear minimum variance unbiased estimator. According to pp. 147–148 of Ref. [8], it follows that

$$\hat{\boldsymbol{q}}=(\boldsymbol{B}^{\mathrm{T}}\cdot C_\mu^{-1}\cdot\boldsymbol{B})^{-1}\cdot\boldsymbol{B}^{\mathrm{T}}\cdot C_\mu^{-1}\cdot\boldsymbol{\xi} \tag{11a}$$

$$\boldsymbol{C}_e=(\boldsymbol{B}^{\mathrm{T}}\cdot C_\mu^{-1}\cdot\boldsymbol{B})^{-1} \tag{11b}$$

where $\hat{\boldsymbol{q}}$ is a vector representing the difference between the actual and the estimated value of the parameter vector:

$$\begin{aligned}\hat{\boldsymbol{q}}&=\boldsymbol{p}-\hat{\boldsymbol{p}}\\&=(s_x-\hat{s}_x,\ s_y-\hat{s}_y,\ s_z-\hat{s}_z,\ o_x-\hat{o}_x,\ o_y-\hat{o}_y,\ o_z-\hat{o}_z)\end{aligned} \tag{12}$$

$\boldsymbol{B}$ is a vector representing the partial derivative of the mathematical model with respect to its parameters, substituting the previous estimate of the parameter vector:

$$\begin{aligned}\boldsymbol{B}=\frac{\partial h(\boldsymbol{v},\boldsymbol{p})}{\partial \boldsymbol{p}}\bigg|_{\boldsymbol{p}=\hat{\boldsymbol{p}}(-)}= & -\frac{(v_x-\hat{o}_x(-))^2}{r\cdot\hat{s}_x^3(-)}\\ & -\frac{(v_y-\hat{o}_y(-))^2}{r\cdot\hat{s}_y^3(-)}-\frac{(v_z-\hat{o}_z(-))^2}{r\cdot\hat{s}_z^3(-)}-\frac{v_x-\hat{o}_x(-)}{r\cdot\hat{s}_x^2(-)}\\ & -\frac{v_y-\hat{o}_y(-)}{r\cdot\hat{s}_y^2(-)}-\frac{v_z-\hat{o}_z(-)}{r\cdot\hat{s}_z^2(-)}\end{aligned} \tag{13a}$$

with

$$r=\sqrt{\frac{v_x-\hat{o}_x(-)}{\hat{s}_x(-)}^2+\frac{v_y-\hat{o}_y(-)}{\hat{s}_y(-)}^2+\frac{v_z-\hat{o}_z(-)}{\hat{s}_z(-)}^2} \tag{13b}$$

ξ is a scalar representing the difference between the measured and estimated output of the system:

$$\begin{aligned}\xi&=y-h(\boldsymbol{v},\hat{\boldsymbol{p}}(-))=1[g]\\&-\sqrt{\frac{v_x-\hat{o}_x(-)}{\hat{s}_x(-)}^2+\frac{v_y-\hat{o}_y(-)}{\hat{s}_y(-)}^2+\frac{v_z-\hat{o}_z(-)}{\hat{s}_z(-)}^2}\end{aligned} \tag{14}$$

C_μ is the variance matrix of the measurement noise μ and $\boldsymbol{C}_e$ is the error matrix which represents the mismatch between the real and the estimated value of the parameter vector.

By expanding ξ and $\boldsymbol{B}$ from one measurement to n measurements (which implies that the dimension of ξ expands to a $1\times n$ vector and the dimension of $\boldsymbol{B}$ expands to a $6\times n$ matrix), the vector $\boldsymbol{\xi}$ and the matrix $\boldsymbol{B}$ are obtained, as desired for Eqs. (11a) and (11b). Now, by constructing $\boldsymbol{\xi}$ and $\boldsymbol{B}$ from the measured values of the output voltages $\boldsymbol{v}$, the change of the parameters can be calculated. The error matrix $\boldsymbol{C}_e$ gives an indication of the variance of the estimated parameters. For C_μ the variance of the collection of quasi-static moments is used, where it is assumed that the variance of the collection of quasi-static moments is constant.

Summarizing, a tool is created with which it is possible to obtain the parameters s_x, s_y, s_z, o_x, o_y and o_z from a collection of quasi-static voltages. So, given the previous estimates of the parameters and a collection of quasi-static moments, it is possible to find the best estimates for the given collection by using the parameter estimator. The parameter estimator can be used to estimate either all parameters or the offsets only, in case the sensitivities are assumed to be known and stable.

It is not likely that during daily life movements are made in such a way that the collection of quasi-static moments is equal to the collection of all possible static moments. Instead, it is expected that a part of the ellipsoid as shown in Fig. 4(b) is more likely to occur. It is anticipated that the accuracy of the estimated parameters is related to the part of the ellipsoid that is known and this relation is examined in the following section.

3. Experimental

The proposed calibration procedure was tested with three commercially available uniaxial accelerometers (ICSensors 3021-010-P) which are placed mutually orthogonal on a box. For the orientation of the sensor with respect to the body of the patient, two different orientations were chosen, as shown in Fig. 5. The triaxial accelerometer can possibly be placed at the lower back of the patient [10]. In that case, for orientation 1, the z-axis of the sensor is parallel to gravity when the patient is standing; for orientation 2, gravity is equally distributed over the three axes when the patient is standing.

Although orientation 1 is the most obvious one, it has the disadvantage that the output voltage of the z-axis, v_z, will hardly show any variation during normal daily life, which may cause a large error in the estimated values of the parameters. Since gravity is equally distributed over the three axes, orientation 2 should not have this disadvantage. This assumption will be verified in the next section.

The part of the ellipsoid that occurs during the activities of daily living (ADL) in a patient with the sensor at his lower back in orientation 1 can be represented with one single parameter, namely the maximum angle with respect to gravity, θ, which is shown in Fig. 6. It is assumed that the most occurring posture is standing or sitting ($a_z = 1g$, $a_x = 0$, $a_y = 0$ in the orientation of Fig. 5(a)) and that other occurring postures are spread symmetrically as indicated in Fig. 6.

Two relations were examined, both by simulations and measurements and both for estimating all parameters and estimating the offsets only. The errors in the estimated parameters as a function of the angle θ for both orientations of the sensor were analysed.

For the simulations, the necessary collections of quasi-static moments were created by randomly generating samples over the part of the ellipsoid that was examined (limited by θ). The diagonal elements of the variance matrix C_μ of the measurement noise μ were set to 0.05. For the measurements, the necessary collections were created by manually moving the sensor (thus describing the desired part of the ellipsoid) whilst the output voltages were recorded using a LabView facility. The threshold value T_v of the quasi-static moments detector was set at $T_v = 0.40$ V [7]. Each in-use calibration was preceded by a reference calibration according to Ref. [9].

By comparing the parameters obtained by both calibration methods, the propagation of the errors in the parameters into the estimated acceleration can be calculated. The relative error in the estimated acceleration due to inaccuracies in the estimated offset is called $\mathrm{error}_{\mathrm{offset}}$ [% of $1g$] and the relative error in the estimated acceleration due to inaccuracies in the estimated sensitivity is called $\mathrm{error}_{\mathrm{sensitivity}}$ [% of $1g$]. The relative errors can be given as

$$\mathrm{error}_{\mathrm{offset}} = \frac{|o_{\mathrm{estimated,dir}} - o_{\mathrm{actual\ value,dir}}|}{s_{\mathrm{actual\ value,dir}}} \cdot 100\% \qquad (15)$$

$$\mathrm{error}_{\mathrm{sensitivity}} = \frac{|s_{\mathrm{estimated,dir}} - s_{\mathrm{actual\ value,dir}}|}{s_{\mathrm{actual\ value,dir}}} \cdot 1[g] \cdot 100\% \quad \text{at } 1g \qquad (16)$$

It is chosen to express the relative error in the estimated acceleration as a percentage of $1g$ because that clearly shows the influence of the error on the values of the accelerations as calculated from the measured output voltages. It should be noted that $\mathrm{error}_{\mathrm{sensitivity}}$ is dependent on the actual acceleration, so $\mathrm{error}_{\mathrm{sensitivity}} = 0$ at $0g$ and is 10 times as high at $10g$ as it is at $1g$.

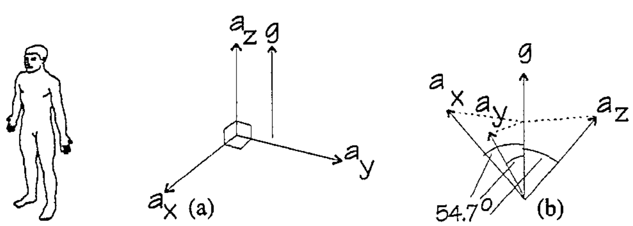

Fig. 5. Representation of the orientation of the sensor with respect to the body when the sensor is placed at the lower back of the patient and the patient is standing: (a) orientation 1, the z-axis parallel to gravity; (b) orientation 2, gravity equally distributed over the three axes.

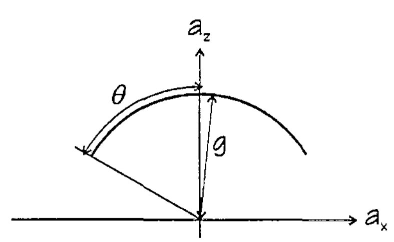

Fig. 6. Two-dimensional representation of the part of the ellipsoid that occurs during activities of daily living in a patient with the triaxial accelerometer at his lower back.

4. Results and discussion

The measurement results for the two sensor orientations as shown in Fig. 5 are displayed in Figs. 7–9 and Figs. 10–12, respectively. It was chosen to display the relative errors in the estimated acceleration for both all parameters and offsets only, because the offsets were found to drift much more than

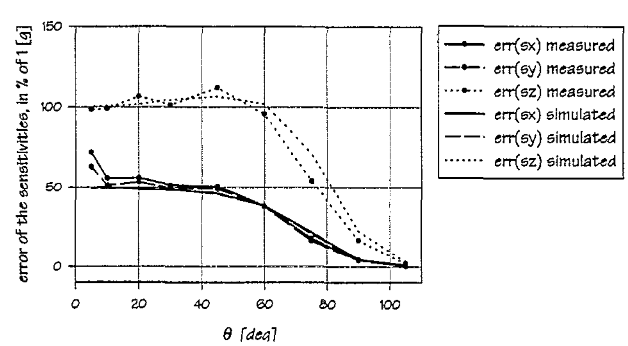

Fig. 7. Relative error in the estimated acceleration due to inaccuracies in the estimated sensitivities vs. θ, for estimating all parameters with orientation 1.

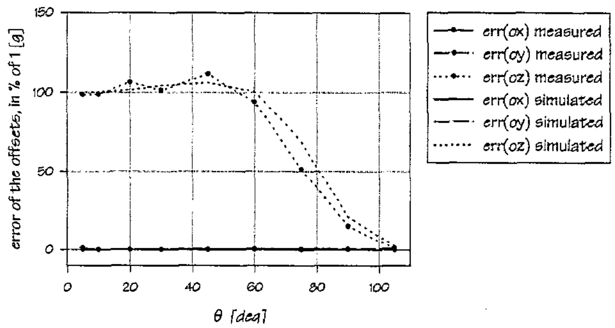

Fig. 8. Relative error in the estimated acceleration due to inaccuracies in the estimated offsets vs. θ, for estimating all parameters with orientation 1.

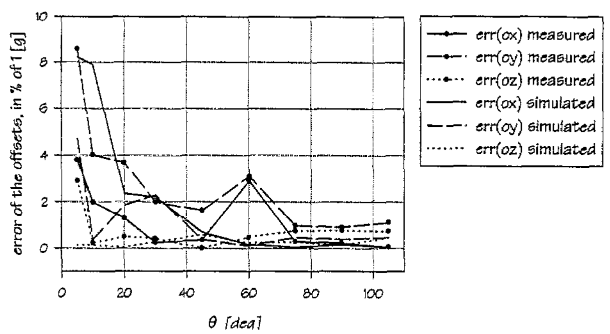

Fig. 9. Relative error in the estimated acceleration due to inaccuracies in the estimated offsets vs. θ, for estimating offsets only with orientation 1; note the scale of the y-axis.

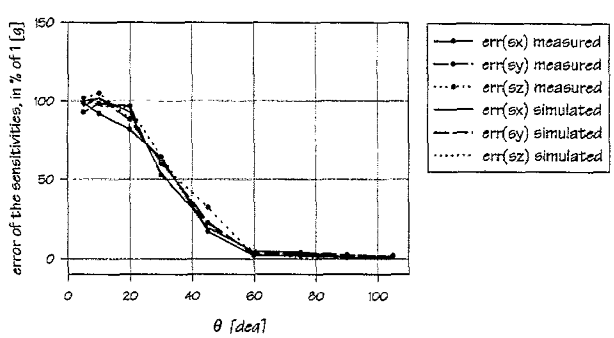

Fig. 10. Relative error in the estimated acceleration due to inaccuracies in the estimated sensitivities vs. θ, for estimating all parameters with orientation 2.

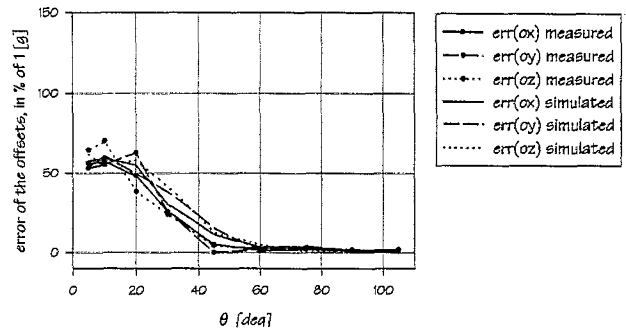

Fig. 11. Relative error in the estimated acceleration due to inaccuracies in the estimated offsets vs. θ, for estimating all parameters with orientation 2.

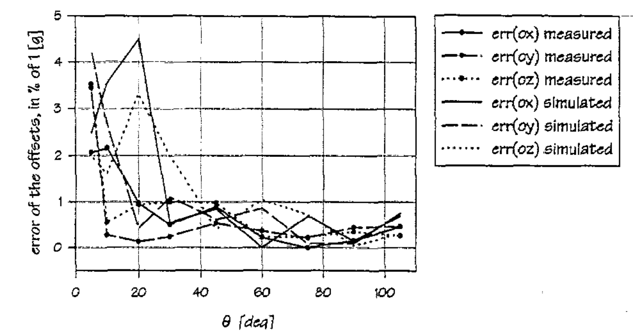

Fig. 12. Relative error in the estimated acceleration due to inaccuracies in the estimated offsets vs. θ, for estimating offsets only with orientation 2; note the scale of the y-axis.

the sensitivities. In Figs. 7 and 10 the errors of the sensitivities are shown for the situation in which all parameters were estimated. In Figs. 8 and 11 the errors of the offsets are shown for the situation in which all parameters were estimated and in Figs. 9 and 12 the errors of the offsets are shown for the situation in which the offsets only were estimated.

In general, it is observed that the measurement results correspond well to the simulation results for both orientations. It can therefore be concluded that the on-line calibration procedure performs as expected by the simulations. It can also be seen that the error of the estimated parameters decreases when θ increases.

For orientation 1, when all parameters are estimated, θ should be larger than 105° to obtain estimates of which the error is smaller than 3%. In a practical situation, this occurs, for instance, when someone is going to bed. When only the offsets are estimated, θ should be larger than 30° to obtain estimates of which the error is smaller than 3%. For orientation 2, it is found that to estimate all parameters with an average error smaller than 3%, θ has to be at least 75°. To estimate the offsets only with an average error smaller than 3%, θ has to be at least 20°. It has to be noted that the movements performed provided enough quasi-static samples to ensure a well-performed calibration. Also, it was assumed that the difference between the previous estimates and the new parameter values was less than 5% to ensure convergence of the estimator.

When the results of the orientation 1 (at which the z-axis is parallel to gravity) are compared to those of orientation 2 (at which gravity is equally distributed over the three axes), it is seen that the errors of the estimated parameters of orientation 2 are smaller than the errors of orientation 1, as was expected: orientation 1 has the disadvantage that the output voltage of the z-axis, v_z, will hardly show any variation during normal daily use, thus causing a large error in the estimated parameter values. Since in orientation 2 gravity is equally distributed over the three axes, orientation 2 does not have this disadvantage and is therefore preferred.

5. Conclusions

A calibration procedure is developed with which it is possible to calibrate the sensitivities and the offsets of a triaxial accelerometer while in use, requiring only random movements as input. The calibration can be performed within several minutes. It was found advantageous to choose the orientation of the sensor with respect to the body in such a way that gravity is equally distributed over the three sensitive axes when the patient is at rest.

Considering practical applications, it was found possible to obtain an average error in the estimated acceleration smaller than 3% with the calibration procedure for inputs caused by 'standing straight and moving slightly' when only the offsets are estimated. For the input caused by a sequence that for instance occurs when going to bed, it was found possible to obtain errors smaller than 3% for estimating all parameters.

Acknowledgements

The authors would like to thank Z. Houkes, associate professor at the University of Twente, for his assistance in understanding the concept of parameter estimation and the Dutch Technology Foundation (STW) for its financial support.

References

[1] D. Marioli, E. Sardini, A. Taroni, A computerized system for the very low frequency calibration of accelerometers, Proc. 6th Int. Symp. Intelligent Instrumentation for Remote and On-Site Measurements, IMEKO TC-4, Antwerp, Belgium, May 1993, pp. 437–442.

[2] C. Estrich, K. Rangan, An automated accelerometer calibration station, Nat. Conf. of Standard Laboratories, 1989, pp. 6–11.

[3] B. Barshan, H.F. Durrant-Whyte, Inertial navigation systems for mobile robots, IEEE Trans. Robotics Automation 11 (3) (1995) 328–342.

[4] M.S. Grewal, V.D. Henderson, R.S. Miyasako, Application of kalman filtering to the calibration and alignment of inertial navigation systems, IEEE Trans. Automatic Control 36 (1991) 4–13.

[5] J. Schipper, J.C. Lötters, P.H. Veltink, W. Olthuis, P. Bergveld, Procedure for in-use calibration of triaxial accelerometers, Tech. Digest, Eurosensors XI, Warsaw, Poland, 21–24 Sept., 1997, pp. 1599–1602.

[6] P.H. Veltink, H.B.J. Bussmann, W. de Vries, W.L.J. Martens, R.C. van Lummel, Detection of static and dynamic activities using uniaxial accelerometers, IEEE Trans. Rehab. Eng. 4 (1996) 375–385.

[7] J. Schipper, The design and realisation of a calibration procedure for in use calibration of the triaxial accelerometer, M.Sc. Thesis, University of Twente, 1997, pp. 16–20.

[8] P.B. Liebelt, An Introduction to Optimal Estimation, Addison-Wesley, Reading, MA, 1967, pp. 148-150.

[9] F. Ferraris, U. Grimaldi, M. Parvis, Procedure for effortless in-field calibration of three-axis rate gyros and accelerometers, Sensors Mater. 7 (5) (1995) 311–330.

[10] C.T.M. Baten, P. Oosterhoff, I. Kingma, P.H. Veltink, H.J. Hermens, Inertial sensing in ambulatory load estimation, Proc. Eng. Med. Biol. Soc., 18th Ann. Int. Conf., Amsterdam, The Netherlands, 31 Oct.–3 Nov., 1996, 2 pp. on CD ROM.

Biographies

Joost C. Lötters was born in Doetinchem, The Netherlands, on 20 July, 1967. In 1990, he received the B.Sc. degree in electrical engineering from the Technical Institute Arnhem, Arnhem, The Netherlands, in 1993 the M.Sc. and in 1997 the Ph.D. degree in electrical engineering from the University of Twente, Enschede, The Netherlands. The title of his Ph.D. thesis is 'A highly symmetrical capacitive triaxial accelerometer', and it deals with the design and fabrication of a miniature and eventually implantable triaxial accelerometer for biomedical purposes. Possible applications of the device are the control of mobility in paraplegic patients and the monitoring of movement disorders of patients suffering from Parkinson's disease. In 1997, he joined the research department of Bronkhorst High-Tech, Ruurlo, The Netherlands.

Jeroen Schipper was born in Zwolle, The Netherlands, in 1971. In 1997, he received the M.Sc. degree in electrical engineering from the University of Twente, Enschede, The Netherlands. His M.Sc. thesis dealt with the design of a calibration procedure for in-use calibration of a triaxial accelerometer. In 1997, he joined the customer services division of Ericsson Business Mobile Networks, Enschede, The Netherlands.

Peter H. Veltink studied electrical engineering at the University of Twente, The Netherlands, where he received the M.Sc degree in 1984 and the Ph.D. degree in 1988 (dissertation: recruitment of myelinated nerve fibres during artificial nerve stimulation). Currently, he is a member of the Biomedical Engineering Division of the Department of Electrical Engineering, University of Twente, and is engaged in the research of neuromuscular stimulation for rehabilitation of spinal cord injured patients and the application of inertial sensors for human movement analysis, which is carried out in cooperation with the Roessingh rehabilitation centre in Enschede. His research interests are artificial motor control, signal processing and measurement technology for sensor systems.

Wouter Olthuis was born in Apeldoorn, The Netherlands, on 23 Oct., 1960. He received the M.Sc. degree in electrical engineering from the University of Twente, Enschede, The Netherlands, in 1986, and the Ph.D. degree from the Biomedical Engineering Division of the Faculty of Electrical Engineering, University of Twente, in 1990. The subject of his dissertation was the use of iridium oxide in ISFET-based coulometric sensor–actuator devices. Currently he is working as an assistant professor in the Biosensor Technology Group, part of the MESA Research Institute of the University of Twente.

Piet Bergveld was born in Oosterwolde, The Netherlands, on 26 January, 1940. He received the M.Sc. degree in electrical engineering from the University of Eindhoven, The Netherlands, in 1965 and the Ph.D. degree from the University of Twente, The Netherlands, in 1973. The subject of his dissertation was the development of ISFETs and related devices, the actual invention of the ISFET, since then also investigated by many international research groups of universities as well as industry. Since 1965 he has been a member of the Biomedical Engineering Division of the Faculty of Electrical Engineering (University of Twente) and was in 1984 appointed as full professor in biosensor technology. He is one of the project leaders in the MESA Research Institute. His research subjects still concern the further development of ISFETs and biosensors based on ISFET technology as well as physical sensors for biomedical and environmental applications, resulting up to now in more than 250 papers. He recently became a member of the KNAW, a committee for advising the Dutch government.